



R. J. Adrian · D. F. G. Durão · F. Durst
M. Maeda · J. H. Whitelaw (Eds.)

Applications of Laser Techniques to Fluid Mechanics

5th International Symposium
Lisbon, Portugal, 9-12 July, 1990

With 358 Figures

Springer-Verlag
Berlin Heidelberg New York
London Paris Tokyo
Hong Kong Barcelona Budapest

Professor R. J. Adrian
University of Illinois
Talbot Laboratory 216
104 Wright Street
Urbana IL 61801
USA

Professor M. Maeda
Keio University
Mechanical Engineering Dept.
3-14-1 Hiyoshi
Kohoko-ku
Yokohama 223
Japan

Professor D. F. G. Durão
Instituto Superior Tecnico
Av. Rovisco Pais
Lisbon
Portugal

Professor J. Whitelaw
Imperial College
Mechanical Engineering Dept.
Exhibition Road
London SW7 2BX
England

Professor F. Durst
University of Erlangen-Nürnberg
Dept. of Fluid Mechanics
Cauerstraße 4
8520 Erlangen
Germany

ISBN-13:978-3-642-64763-5 e-ISBN-13:978-3-642-61254-1
DOI: 10.1007/978-3-642-61254-1

Library of Congress Cataloging-in-Publication Data
International Symposium on Applications of Laser Techniques to Fluid Mechanics
(5th : 1990 : Calouste Gulbenkian Foundation)
Applications of laser techniques to fluid mechanics
5th international symposium, Lisbon, Portugal, 9-12 July 1990 / R. J. Adrian ... [et al.].
"Papers selected from the proceedings of the Fifth International Symposium
on Applications of Laser Techniques to Fluid Mechanics,
held at the Calouste Gulbenkian Foundation in Lisbon from 9 to 12 July 1990"--Pref.
ISBN-13:978-3-642-64763-5

1. Fluid dynamic measurements--Congresses. 2. Lasers--Congresses.

I. Adrian, R. J. (Ronald J.)
TA357.5.M43I58 1990 681'.2--dc20 91-26951

This work is subject to copyright. All rights are reserved, whether the whole or part of the material is concerned, specifically the rights of translation, reprinting, re-use of illustrations, recitation, broadcasting, reproduction on microfilms or in any other way, and storage in data banks. Duplication of this publication or parts thereof is only permitted under the provision of the German Copyright Law of September 9, 1965, in its current version and permission for use must always be obtained from Springer-Verlag. Violations are liable for prosecution under the German Copyright Law.

© Springer-Verlag Berlin, Heidelberg 1991
Softcover reprint of the hardcover 1st edition 1991

The use of registered names, trademarks, etc. in this publication does not imply, even in the absence of a specific statement, that such names are exempt from the relevant protective laws and regulations and therefore free for general use.

Typesetting: Camera ready by authors;

2161/3020-543210 - Printed on acid-free paper.

Preface

This volume consists of papers selected from the proceedings of the Fifth International Symposium on Applications of Laser Techniques to Fluid Mechanics, held at the Calouste Gulbenkian Foundation in Lisbon from 9 to 12 July, 1990. Relative to previous meetings in the Lisbon series the scope of this symposium was broadened by expanding the topical coverage to include all laser techniques used in fluid mechanics. This change recognized the trend amongst experimental fluid dynamicists to employ laser techniques for the measurement of many different quantities, including concentration, temperature, particle size, and velocity, and the need for researchers to have a forum in which to communicate their work and share their common interests. The Fifth Symposium contained twenty-three sessions of formal presentations and a lively Open Forum session. In addition, Dr. H. J. Pfeiffer organized a special Workshop on the Use of Computers in Flow Measurements which contained five sessions on frequency domain processors, correlators, special detectors, and biasing.

The Editors of this volume were assisted in organizing the Symposium by members of an Advisory Committee, listed on the following page, whose valuable services as referees of abstracts and as chairmen of technical sessions are greatly appreciated. We are also grateful to the authors and to the other participants of the Symposium for the contributions they made. Financial support of the Symposium, which was essential to its success, was provided by the following organizations:

Centro de Termodinâmica Aplicada e Mecânica dos Fluidos da Universidade Técnica de Lisboa

Commission of the European Communities

Direcção Geral de Turismo

European Research Office: United States Army, Navy and Air Force

Fundação Luso-Americana para o Desenvolvimento

Fundação Calouste Gulbenkian

Instituto Nacional de Investigação Científica

Instituto Superior Técnico

Junta Nacional de Investigação Científica e Tecnológica

Sociedade Estoril Sol, SARL

TAP—Air Portugal

The organization of this volume reflects coherent areas that were prominent at the symposium: scalar transport, two-phase flow, instrumentation, and whole field techniques. We wish to thank all of the authors for contributing their papers and for their efforts in preparing the manuscripts.

Urbana, April 1991

The Editors

Advisory Committee

A. D'Alessio, Università di Napoli, Naples, Italy
W. D. Bachalo, Aerometrics, Inc., CA, USA
A. Boutier, ONERA, Chantillon, France
V. Brederode, Instituto Superior Técnico, Lisbon, Portugal
A. Coghe, CNPM-CNR, Milano, Italy
D. Dopheide, Physikalische-Techn. Bundesanstalt, Germany
L. E. Drain, Reading, England
R. V. Edwards, Case Western Reserve University, OH, USA
H. Eickhoff, DRL, Koln, Germany
M. P. Escudier, University of Liverpool, England
A. F. de O. Falcão, Instituto Superior Técnico, Lisbon, Portugal
L. M. Fingerson, TSI, Inc., MN, USA
G. Gouesbet, Laboratoire de Thermod., Université de Rouen, France
K. Hanjalic, University of Sarajevo, Yugoslavia
M. V. Heitor, Instituto Superior Técnico, Lisbon, Portugal
D. Hirleman, Arizona State University, AZ, USA
J. A. C. Humphrey, University of California, Berkeley, USA
R. Karlsson, Swedish State Power Board, Alvkarleby, Sweden
L. Lading, Danish Atomic Energy Research, Riso, Denmark
B. Lehmann, DLR, Berlin, Germany
A. Melling, AVL-LIST, Graz, Austria
W. Merzkirch, Universität Essen, Germany
J. F. Meyers, NASA-Langley Research Center, VA, USA
A. Muller, Eidgenossische Technische Hochschule, Zurich, Switzerland
N. Nakatani, Osaka University, Osaka, Japan
M. N. R. Nina, Instituto Superior Técnico, Lisbon, Portugal
K. Ohba, Kansai University, Osaka, Japan
T. Obokata, Gunma University, Kiryu, Japan
J. C. F. Pereira, Instituto Superior Técnico, Lisbon, Portugal
H. J. Pfeifer, Ins. Franco Allemand de Rech. de Saint-Louis, France
P. A. Pfund, Babcock & Wilcox, OH, USA
A. Restivo, Universidade do Porto, Porto, Portugal
W. C. Reynolds, Stanford University, CA, USA
M. L. Riethmuller, Von Karman Inst. Fl. Dyn., Rhode-St.-Genese, Belgium
R. L. Simpson, Virginia Polytechnic Inst. and State Univ., VA, USA
X. Shen, Tsinghua University, Beijing, China
W. L. Stevenson, Purdue University, IN, USA
N. Syred, University College, Cardiff, Wales
A. M. K. P. Taylor, Imperial College, London, England
C. Tropea, Universität Erlangen, Erlangen, Germany
J. T. Turner, University of Manchester, England
C. Wigley, AVL-LIST, Graz, Austria
P. O. Witze, Sandia National Laboratories, CA, USA

Table of Contents

Chapter I – SCALAR TRANSPORT

Four-Dimensional Laser Induced Fluorescence Measurements of Conserved Scalar Mixing in Turbulent Flows W. J. A. Dahm, K. B. Southerland and K. A. Buch	3
Planar Laser-Induced Fluorescence Scalar Measurements in a Turbulent Jet A. Lozano, I. J. van Cruyningen and R. K. Hanson	19
Simultaneous Measurement of Velocity and Temperature of Water Using LDV and Fluorescence Technique T. Nakajima, M. Utsunomiya, Y. Ikeda and R. Matsumoto	34
Simultaneous, Real-Time Line Measurements of Concentration and Velocity in Turbulent Flows K. C. Muck, J. M. Wallace and W. M. Pitts	54
Digital Particle Image Thermometry and Its Application to a Heated Vortex-Ring D. Dabiri and M. Gharib	81
Temperature Measurement in a Asymmetric Thermal Flow Field by Laser Holographic Interferometry S.-M. Tieng and H.-T. Chen	102

Chapter II – TWO-PHASE FLOW, SIZE AND VELOCITY

LDA Measurements of Plastic and Elastic Collisions of Small Particles with Metal Surfaces S. R. Martin, T. M. Pinfeld and G. R. Wallace-Sims	125
The Influence of Swirl on the Particle Dispersion in a Pipe Expansion Flow M. Sommerfeld, H.-H. Qiu and D. Koubaridis	142
Flow Measurements in a Liquid Fuelled Burner D. F. G. Durão, M. V. Heitor and A. L. N. Moreira	163
Fringe Count Limitations on the Accuracy of Velocity and Mass Flux in Two-Phase Flows Y. Hardalupas, A. M. K. P. Taylor and J. H. Whitelaw	183
Measurement of Size and Velocity Distributions of Droplets Produced by Bubbles Bursting M. Ramirez De Santiago and C. Marvillet	203
Sensitivity of Dropsizes Measurements by Phase Doppler Anemometry to Refractive Index Changes in Combusting Fuel Sprays G. Pitcher, G. Wigley and M. Saffman	227
LDA Measurement of Gasoline Droplet Velocities and Sizes at Intake-Valve Annular Passage in Steady Flow State H. Kawazoe, K. Ohsawa and M. Kataoka	248
Measurement of Fuel Injector Spray Flow of I. C. Engine by FFT Based Phase Doppler Anemometer — An Approach to the Time Series Measurement of Size and Velocity K. Kobashi, K. Hishida and M. Maeda	268

Chapter III – INSTRUMENTATION

Signal Processing Considerations for Laser Doppler and Phase Doppler Applications K. M. Ibrahim, G. D. Werthimer and W. D. Bachalo	291
Improved Optical Systems for Velocimetry and Particle Sizing Using Semiconductor Lasers and Detectors J. Domnick, F. Durst, R. Müller and A. Naqwi	317
A Photothermal Velocimeter Using an Optical Fibre Heterodyne Interferometer with Phase Differentiation at Two Points N. Nakatani, T. Oshio, J. Inagaki, T. Kataoka and K. Kishida	331
Two-Point Adapter for LDA Probe Using Multimode Fibers T. Obokata, S. Bopp and C. Tropea	347
Velocity Measurement Using Fibre Optic Sagnac Interferometers R. McBride, D. Harvey, J. S. Barton and J. D. C. Jones	364
Semiconductor Long-Range Anemometer Using a 5 mW Diode Laser and a Pin Photodiode D. Dopheide, M. Faber, Yen-Bing-u and G. Taux	385
An Experimental Evaluation of a Novel Method of Using Localized Laser Heating in the Determination of Wall Shear Stress W. E. Carscallen, P. H. Oosthuizen and F. J. Arthur	400

Chapter IV – WHOLE-FIELD VELOCIMETRY

Application of Particle Image Velocimetry to Transonic Flows R. Höcker and J. Kompenhans	415
Studies of Liquid Turbulence Using Double-Pulsed Particle Correlation R. J. Adrian, P. W. Offutt, T. J. Hanratty, Z.-C. Liu and C. C. Landreth	435
Turbulent Intensity Evaluation with PIV A. Cenedese, G. Palmieri and G. P. Romano	451
Instantaneous Particle Image Velocimetry with Electronic Specklegram E. Okada, H. Enomoto, Y. Fukuoka and H. Minamitani	464
Measurement of Dynamics of Coherent Flow Structures Using Particle Image Velocimetry J. Westerweel, F. T. M. Nieuwstadt and J. B. Flor	476
Two-Phase Flow Velocity Measurements Using Automated-Based Imaging Pulsed Laser Velocimetry Y. Hassan and T. Blanchat	500
Mixing Flow in a Cylindrical Vessel Agitated by a Bubbling Jet —Application of Image Processing Velocimetry T. Uémura, K. Ohmi and F. Yamamoto	521
Visualization and Measurement of Detailed Velocity Field in U-Bend and Branched Tube Using Laser-Induced Fluorescence Method K. Ohba, A. Sakurai, M. Sato and S. Sakaguchi	537
Photobleaching Flow Visualization K. F. Sollows, C. R. Dutcher, A. C. M. Sousa and J. E. S. Venart	553

Scalar Transport

Four-Dimensional Laser Induced Fluorescence Measurements of Conserved Scalar Mixing in Turbulent Flows

Werner J.A. Dahm, Kenneth B. Southerland and Kenneth A. Buch

Department of Aerospace Engineering
The University of Michigan
Ann Arbor, Michigan, USA

Abstract

We deal with conserved scalar mixing in turbulent flows, and present a newly developed laser imaging diagnostic for obtaining highly detailed, four-dimensional measurements of the full space and time varying conserved scalar field $\zeta(\mathbf{x},t)$ and the associated scalar energy dissipation rate field $\nabla\zeta \cdot \nabla\zeta(\mathbf{x},t)$ in a turbulent flow. The method is based on high-speed, high-resolution, successive planar laser induced fluorescence imaging of a synchronized raster swept laser beam, combined with high-speed data acquisition of gigabyte-sized data sets using very fast computer disk ranks. The measurement resolution reaches down to the local strain-limited molecular diffusion scale in the flow, so that the resulting four-dimensional data are directly differentiable in all three space dimensions and in time. These data spaces are numerically analyzed to determine the time evolution of all three components of the instantaneous scalar gradient vector field $\nabla\zeta(\mathbf{x},t)$ and the resulting instantaneous scalar energy dissipation rate field. Typical results are presented in the form of spatial sequences of adjacent two-dimensional data planes within a particular three-dimensional data volume, as well as temporal sequences of spatial data planes from three-dimensional data volumes acquired successively in time, allowing the evolution of the true scalar dissipation rate to be examined in detail throughout the four-dimensional data space.

Introduction

The problem of mixing of conserved scalar quantities in turbulent flows can be formally posed in terms of a conserved scalar field $\zeta(\mathbf{x},t)$ which satisfies the advection-diffusion equation

$$\left[\frac{\partial}{\partial t} + \mathbf{u} \cdot \nabla - \frac{1}{ReSc} \nabla^2 \right] \zeta(\mathbf{x},t) = 0. \quad (1)$$

The associated scalar energy per unit mass $1/2\zeta^2(\mathbf{x},t)$, defined analogous to the kinetic energy per unit mass $1/2\mathbf{u}^2(\mathbf{x},t)$, where $\mathbf{u} \equiv |\mathbf{u}|$, can then be shown from Eq. (1) to follow the exact transport equation

$$\left[\frac{\partial}{\partial t} + \mathbf{u} \cdot \nabla - \frac{1}{ReSc} \nabla^2 \right] \frac{1}{2} \zeta^2(\mathbf{x},t) = - \frac{1}{ReSc} \nabla\zeta \cdot \nabla\zeta(\mathbf{x},t), \quad (2)$$

in which the instantaneous rate of scalar energy dissipation per unit mass $(ReSc)^{-1}\nabla\zeta\cdot\nabla\zeta(\mathbf{x},t)$ gives the rate at which non-uniformities in the scalar energy field are reduced by molecular diffusion at any point in the flow. In this sense, the scalar dissipation field $\nabla\zeta\cdot\nabla\zeta(\mathbf{x},t)$ gives the local instantaneous rate of molecular mixing in the flow. Sometimes the scalar gradient magnitude $|\nabla\zeta(\mathbf{x},t)|$ is adopted as an alternative definition for the local instantaneous molecular mixing rate, though in terms of the logarithm of the mixing rate field these two definitions of course differ only by a constant scale factor.

In the context of the above discussion, the structure of the scalar energy dissipation rate field in turbulent flows is of direct interest in problems involving the mixing of dynamically passive scalar quantities in such flows. However, even in chemically reacting turbulent flows, under certain conditions simultaneous measurements of the conserved scalar field $\zeta(\mathbf{x},t)$ and the associated scalar energy dissipation rate field $\nabla\zeta\cdot\nabla\zeta(\mathbf{x},t)$ allow determination of the structure of the chemical reaction rate field using a formulation first noted by Bilger (1976). In particular, the mass fraction of any chemical species Y follows an advection-diffusion-reaction equation of the form

$$\left[\frac{\partial}{\partial t} + \mathbf{u} \cdot \nabla - \nabla \cdot \frac{1}{ReSc_i} \nabla \right] Y_i(\mathbf{x},t) = \dot{w}_i(\mathbf{x},t). \quad (3)$$

where $\dot{w}_i(\mathbf{x},t)$ is the local instantaneous reaction rate field of species i , and where $ReSc$ is the temperature dependent diffusivity of this species. If the relevant chemical reaction time scales involved in $\dot{w}_i(\mathbf{x},t)$ are sufficiently short in comparison with the local fluid dynamic time scales of the flow, so that the relevant forward and backward reactions involving Y_i remain essentially in equilibrium, then Y_i can be related to an appropriately defined conserved scalar quantity (e.g. the fuel atom mixture fraction) as $Y_i(\mathbf{x},t) = Y_i^{eq}[\zeta(\mathbf{x},t)]$. In that case, Eq. (3) yields

$$\left\{ \left(\frac{dY_i^{eq}}{d\zeta} \right) \left[\frac{\partial}{\partial t} + \mathbf{u} \cdot \nabla - \nabla \cdot \frac{1}{ReSc_i} \nabla \right] \zeta(\mathbf{x},t) \right\} - \left\{ \frac{1}{ReSc_i} \nabla\zeta \cdot \nabla\zeta(\mathbf{x},t) \left(\frac{d^2Y_i^{eq}}{d\zeta^2} \right) \right\} = \dot{w}_i(\mathbf{x},t). \quad (4)$$

If, furthermore, the diffusivities of the scalar ζ and the species i are the same, then from Eq. (1) the first term on the left in Eq. (4) will vanish. The reaction rate field $\dot{w}_i(\mathbf{x},t)$ is then given by

$$\dot{w}_i(\mathbf{x},t) = - \frac{1}{ReSc} \nabla\zeta \cdot \nabla\zeta(\mathbf{x},t) \left(\frac{d^2Y_i^{eq}}{d\zeta^2} \right), \quad (5)$$

namely as the product of the instantaneous scalar dissipation rate field $\nabla\zeta\cdot\nabla\zeta(\mathbf{x},t)$ and the second derivative of the equilibrium relation evaluated at the local instantaneous scalar value $\zeta(\mathbf{x},t)$.

Correspondingly, the concepts of scalar energy and its dissipation rate play a central role in many approaches for understanding and modeling both molecular mixing and chemical reactions in turbulent flows. However, direct measurements of instantaneous scalar dissipation rate

fields in turbulent flows have been difficult to obtain. This has been principally due to two obstacles. First, determination of the true scalar gradient vector field $\nabla\zeta(\mathbf{x},t)$ and the associated scalar energy dissipation rate field $\nabla\zeta\cdot\nabla\zeta(\mathbf{x},t)$ requires measurement of the conserved scalar field $\zeta(\mathbf{x},t)$ in all three spatial dimensions. Second, since the dissipation rate is obtained by differentiation of the measured conserved scalar field, the spatial and temporal resolution of the original scalar measurements must be high enough to accurately resolve the finest local scales on which spatial gradients in the scalar field are present in the flow. Beyond this, the signal quality of the original scalar field measurements must also be high enough to allow accurate differentiation to determine the scalar dissipation rate field.

Previous Work

A number of different approaches have been used in recent years to obtain accurate measurements of conserved scalar fields in turbulent flows. Almost all of these have made use of various planar laser imaging techniques; a good review of many of these is given by Hanson (1986). Relevant to the present work, Long & Chu (1981) and Escoda & Long (1983) addressed the relatively simple large scale features in the transition region of a turbulent jet using single-plane two-dimensional laser imaging measurements. In a similar laser imaging effort aimed at obtaining the additional information in a third dimension from such measurements, Fourquette & Long (1983) and Yip, Long & Fourquette (1986) used acoustic excitation to produce a phase-locked flow which could then be selectively advanced either in space or in time. Bowman, Lewis, Cantwell & Vandsburger (1988) have used a similar forcing technique in conjunction with laser imaging to examine large scale mixing in the near field vortical structures of an excited jet. This technique of artificially phase-locking the large structures in the jet transition region has also been used by Kychakoff, Paul, Cruyngen & Hanson (1987) to obtain three-dimensional measurements in a topologically simple forced flow. Also of relevance here, Hesselink et al (1983) and Agüf & Hesselink (1988) have digitized ciné frames obtained with a rapidly swept laser sheet to obtain qualitative three-dimensional visualizations of the coarse structure of isoscalar surfaces in the transition region of a coflowing turbulent jet.

These previous measurements have all been primarily aimed at the topologically simple large scale features of transitional flows. The spatial and temporal resolution achieved in them has not been adequate to resolve the fine scale structure of the conserved scalar fields typical of fully developed turbulent flows. As a result, while such measurements have produced useful information about the largest flow scales, they have been unable to yield information with sufficient resolution to allow accurate determination of the scalar gradient field and the resulting molecular mixing process in turbulent flows. Yip & Long (1986) have attempted to extend their measurements based on two-dimensional planar laser imaging to yield three-dimensional scalar gradient

information by imaging from two parallel and closely spaced laser sheets. However, both the sheet spacing and the pixel separation were significantly larger than the local molecular diffusion scale in the flow. Following a somewhat different approach, Yip, Lam, Winter & Long (1987) and Yip, Schmitt & Long (1988) have swept a laser sheet at very high speed through a turbulent flow, in conjunction with very high speed image acquisition over a short duration, to obtain measurements in up to 16 closely spaced parallel planes. Nevertheless, even in these measurements the resolution was sufficient only to yield data at comparatively coarse scales of the flow.

Present Work

Here we present a laser imaging diagnostic for obtaining highly detailed, four-dimensional measurements of the full space- and time-varying conserved scalar field $\zeta(\mathbf{x},t)$ and the associated scalar energy dissipation rate field in turbulent flows. The method is based on high-speed, high-

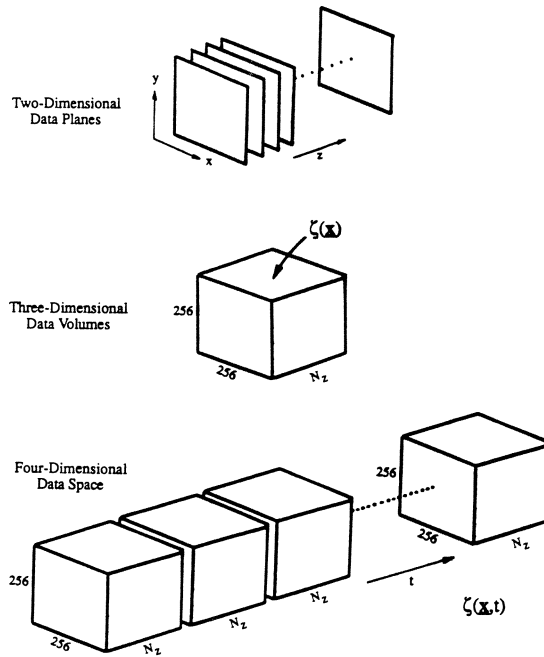


Fig. 1. Structure of the four-dimensional conserved scalar data space $\zeta(\mathbf{x},t)$ as a temporal progression of three-dimensional spatial data volumes, each consisting of a sequence of two-dimensional spatial data planes, each of which consists of a 256×256 array of data points. The spatial and temporal resolution achieved is sufficient to allow direct differentiation of the conserved scalar data in all three space dimensions and in time, allowing the evolution of the true molecular mixing rate field $\nabla\zeta \cdot \nabla\zeta(\mathbf{x},t)$ to be directly determined.

resolution, successive planar laser induced fluorescence imaging of a synchronized raster swept laser beam, combined with high-speed data acquisition of gigabyte sized data sets using very large fast computer disk ranks, to produce a four-dimensional data space structured as shown in Figure 1. Each such measured spatio-temporal data space consists of a rapid progression of individual three-dimensional spatial data volumes, each of which is composed of a sequence of two-dimensional spatial data planes, each consisting of an array of 256×256 individual data points. The spatial separations between adjacent points within each data plane, and also between the adjacent data planes within each data volume, are smaller than the local molecular diffusion scale in the flow. Similarly, the temporal separation between adjacent data planes within each data volume, and between the same data plane in successive data volumes, are shorter than the local molecular diffusion scale advection time. This resolution, together with the high signal quality attained, allows accurate differentiation of the measured conserved scalar data in all three space dimensions and in time. The resulting four-dimensional data volumes are then numerically analyzed to determine the evolution of all three components of the instantaneous scalar gradient vector field $\nabla\zeta(\mathbf{x},t)$ and the resulting true instantaneous scalar energy dissipation rate field $\nabla\zeta \cdot \nabla\zeta(\mathbf{x},t)$. Here we concentrate principally on describing the technique we have developed for acquiring such four-dimensional measurements. A technical discussion of results pertinent to mixing in turbulent flows, obtained from these four-dimensional measurements, is given by Dahm, Southerland & Buch (1990).

Measurement Technique

The technique used and the measurements obtained are an extension of our earlier work (Dahm & Buch 1989, 1991) in developing very high resolution three-dimensional (256^3) spatio-temporal measurements of the conserved scalar concentration field and the resulting scalar energy dissipation rate field in turbulent flows. The present measurements are also based on successive high-speed planar laser induced fluorescence imaging in the self-similar far field of a turbulent shear flow in water. The mixture fraction, in this case determined by the concentration of a passive laser fluorescent dye (disodium fluorescein) carried by one of the fluids, is a conserved scalar in the flow. Here this mixture fraction is measured repeatedly in time throughout a small three-dimensional volume in the flow by imaging the laser induced fluorescence from dye-containing fluid in the path of a laser beam rapidly swept through the volume onto a planar photodiode array. The conserved scalar field $\zeta(\mathbf{x},t)$ can then be obtained from the measured fluorescence intensity through a simple transfer function and attenuation integral as described by Dahm & Buch (1989).

Key elements of the imaging and data acquisition system assembled for these four-dimensional measurements are shown schematically in Figure 2. A pair of very low inertia, galvanometric

mirror scanners are used to synchronously sweep a collimated laser beam in a raster scan fashion through the desired volume in the flow field. The horizontal and vertical sweep angles are typically quite small ($\vartheta_h = 0.125^\circ$ and $\vartheta_v = 4.26^\circ$ for the results presented here). The resulting laser induced fluorescence intensity is measured with a 256×256 imaging array, having a center-to-center pixel spacing of $40 \mu\text{m}$. The array is synchronized to the same clock that drives the scanners, and is driven at variable pixel rates up to 11 MHz, allowing measurement of successive data planes at a continuous rate in excess of 140 planes per second. The fluorescence data from the array is serially acquired through a programmable digital port interface, digitized to 8-bits digital depth, then ported into a 16 MB high-speed, dual-ported data buffer from which it is continuously written in real time to a 3.1 gigabyte high-speed parallel transfer disk rank. The overall sustained data throughput rate to the disks, deducting all the line and frame overhead

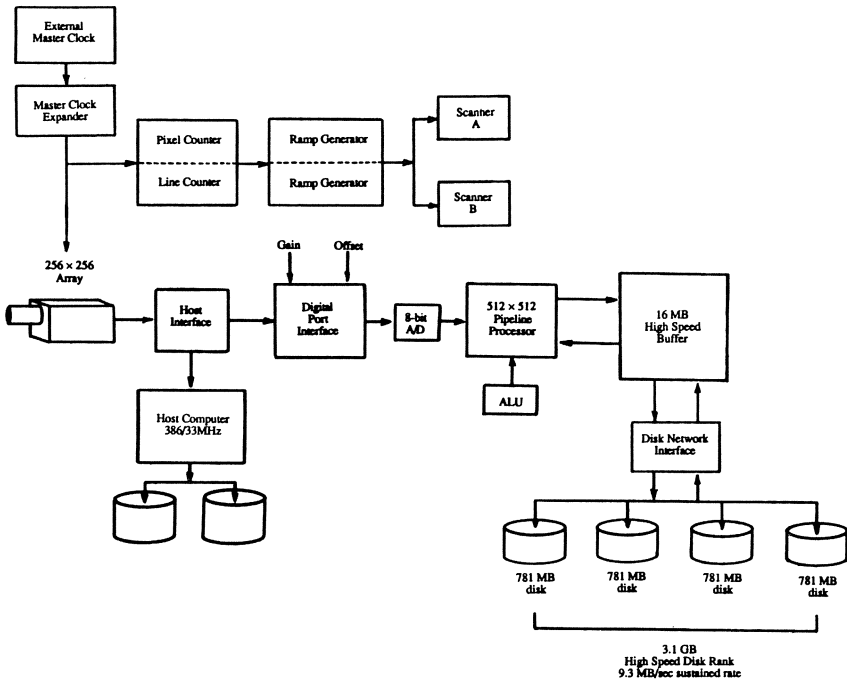


Fig. 2. Key elements of the high-speed, variable-rate (non RS-170) imaging and data acquisition system for obtaining highly-resolved, four-dimensional, laser induced fluorescence measurements of conserved scalar mixing in turbulent flows. Two low-inertia galvanometric laser beam scanners are slaved to the imaging array timing as outlined in Fig. 3 to rapidly sweep the beam in a successive raster fashion through the flow field. The data acquisition system can achieve a sustained throughput rate to the disk bank of up to 9.3 MB/sec for data volumes as large as the full 3.1 GB disk capacity.

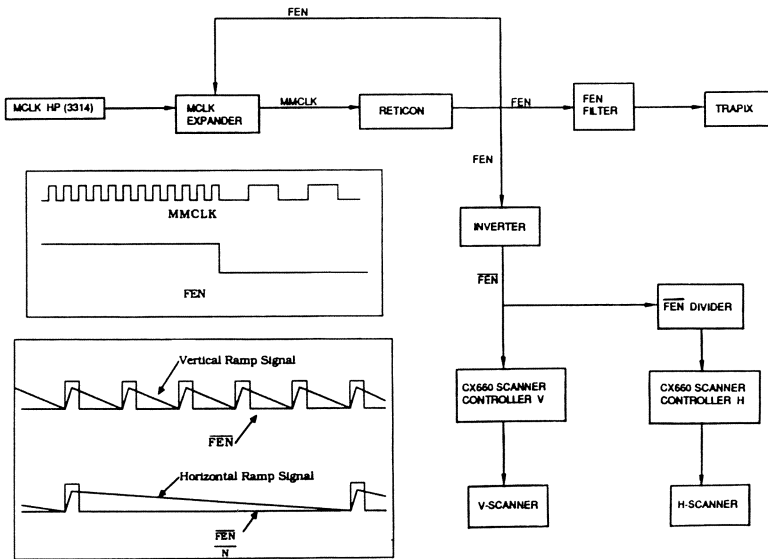


Fig. 3. Schematic overview of the drive and timing electronics for the two laser beam scanners. Each successive vertical sweep of the beam scans through one spatial data plane, while each successive sweep of the horizontal scanner corresponds to one spatial data volume. Acquisition of the data occurs while frame enable (FEN) from the imaging array is high. The scanners are in turn slaved to the imaging array by triggering each of their driver waveforms with the rising edge of FEN and its N_z -period filtered version (FEN/N_z). To accommodate the minimum scanner flyback times, the master clock (MCLK) is temporarily expanded when FEN is low.

cycles, is up to 9.3 MB/sec. The 3.1 GB disk capacity can accommodate more than 50,000 such measured 256×256 spatial data planes within the four-dimensional data space. Programmable gain and offset on the digital port interface allow the resulting data to span the full 8-bits of digital depth. The rms noise levels achieved are in all cases less than ± 1 digital signal level out of the 256 levels spanned by the scalar measurements.

Figure 3 shows the timing arrangement used to synchronize the scanners with the imaging array. Aside from obvious synchronization objectives, the principal concern involves accommodating the minimum flyback times for the scanners within the frame overhead cycles between acquisition of successive data planes, so that each plane will correspond to a single sweep of the beam. Briefly, data acquisition proceeds while frame enable (FEN) from the imaging array is high. FEN goes low during the frame overhead time (nominally 4 line times), which at these clock rates is too short to complete the beam flyback. This requires modifying the original master clock (MCLK) so that, while FEN is low, the clock period is expanded as required for

the frame overhead time to match the minimum flyback time. This modified master clock (MMCLK) then drives both the imaging array and the A/D converter. The resulting FEN and (FEN/N) then respectively drive the vertical (fast) and horizontal (slow) mirror scanners by repeatedly triggering an appropriate ramp waveform for each.

Spatial and Temporal Resolution

Since the principal interest in these measurements is in obtaining the scalar dissipation field from the measured conserved scalar field via direct differentiation of the data, the central issue is the spatial and temporal resolution achieved by the measurements. From the measured thickness of the imaged portion of the laser beam, together with the pixel size and the image ratio of the measurements, the volume in the flow ($\Delta x \cdot \Delta y \cdot \Delta z$) imaged onto each pixel can be determined. Furthermore, for the pixel clock rates used, the time Δt between acquisition of successive data planes within each spatial data volume, and the time ΔT between the same data plane in successive data volumes, can also be determined.

To assess the resulting relative resolution achieved, these smallest spatial and temporal scales discernible in the data must be compared with the finest local spatial and temporal scales on which gradients in the conserved scalar field can be sustained in the flow. For diffusion of vorticity in the presence of a time-varying strain rate $\sigma(t)$, the competing effects of strain and diffusion establish an equilibrium strain-limited vorticity diffusion layer thickness $\lambda_v \sim (\nu/\sigma)^{1/2}$, closely related to the Kolmogorov scale, giving the finest scale on which spatial gradients in the strain rate and vorticity fields can be locally sustained in the flow (e.g. Burgers 1948; Corcos and Sherman 1984). A similar competition between the effects of strain and molecular diffusion of the conserved scalar establishes a local strain-limited molecular diffusion layer thickness $\lambda_D \sim (D/\sigma)^{1/2}$, related to the Batchelor scale and giving the smallest scale on which spatial gradients in the conserved scalar field can be sustained by the flow (e.g. Carrier, Fendell and Marble 1975; Marble 1985). The ratio of the vorticity and scalar diffusivities, ν and D respectively, establishes the relation between these two scales as $\lambda_D \sim \lambda_v \cdot Sc^{-1/2}$, where $Sc \equiv (\nu/D)$ is the Schmidt number and, due to the similarity of the two strain-diffusion equilibrium processes, the proportionality constant should be approximately one. Note that with the highest strain rates occurring locally in the flow scaling as $\sigma \sim (u/\delta) \cdot Re^{1/2}$, the strain-limited diffusion scale in the conserved scalar field is $(\lambda_D/\delta) \sim Sc^{-1/2} Re^{-3/4}$. Measurements by Dowling (1988) give indications that the resulting proportionality constant is roughly 25. Here $Re \equiv u\delta/\nu$ is the local Reynolds number of the shear flow, with $\delta(x)$ and $u(x)$ denoting the local length and velocity scales which characterize the shear at that stage in the flow.

The resolution requirements that Δx , Δy and Δz must be small compared to λ_D to allow differentiation in all three space directions within each three-dimensional spatial data volume, and that

the time ΔT between the same data plane in successive data volumes must be small in comparison with λ_D/u to allow differentiation in time between successive data volumes, ultimately place a limit on the highest Reynolds numbers at which such fully-resolved four-dimensional measurements are possible. Note that while the resolution Δx and Δy within each spatial data plane can in principle be made very small by simply reducing the image ratio, the resolution Δz is nominally determined by the laser beam thickness, and there are clear limitations associated with the Rayleigh range of the laser beam which determine how fine this can be made over the entire extent of the image volume. In general, the resulting minimum laser beam thickness is significantly larger than the desired spatial separation between successive data planes. However, if the time Δt between successive planes is small enough so that the scalar field is effectively frozen, as is the case in all of our measurements, then the overlap in the measured scalar field between adjacent planes represents a convolution of the true scalar field with the laser beam profile, as indicated in Figure 4. The measured scalar field can then be deconvolved with the measured beam profile shape to produce an effective resolution Δz comparable to the spatial separation between adjacent data planes, which is set by the horizontal scanner and can in principle be made arbitrarily small. In the measurements presented here, significant overlap extends only to the next adjacent data plane on either side of each plane, so that the effect of this deconvolution is noticeable but relatively small.

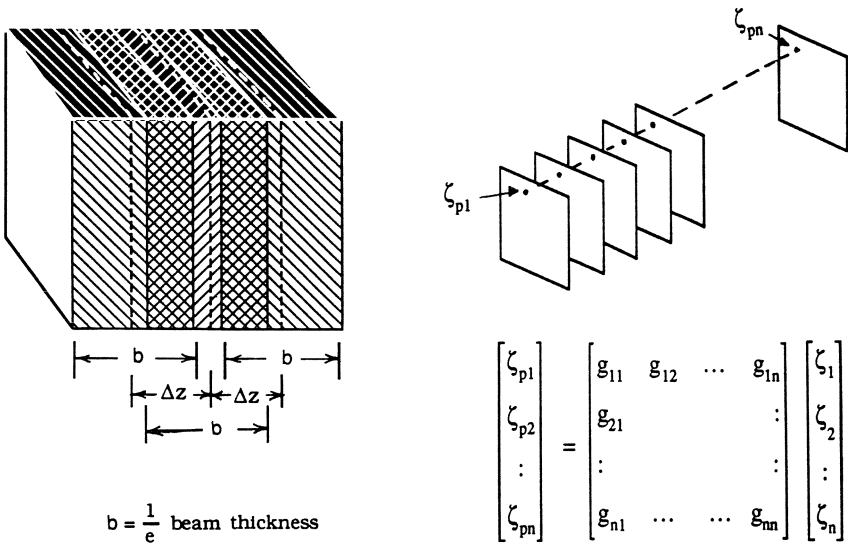


Fig. 4. Schematic showing deconvolution of the measured conserved scalar field between overlapping parallel adjacent spatial data planes to reduce the laser beam thickness resolution limitation, thereby producing an effective z-resolution within each spatial data volume that is comparable to the interplane separation distance, which can be controlled by the scanner driver.

Scalar Dissipation Calculation

From the resulting discrete deconvolved scalar field values in the four-dimensional data space $\zeta_{ijkl} \equiv \zeta(x_i, y_j, z_k, t_l)$, the scalar energy dissipation rate field $(\nabla\zeta \cdot \nabla\zeta)_{ijkl}$ is then obtained by direct differentiation of the data using linear central difference approximations. While any particular choice for the local x-y-z coordinate frame at each point in the volume would make use of only 6 of the 26 scalar values surrounding that point, including other coordinate orientations involves the scalar information at up to all 26 of the surrounding points. Here the scalar dissipation at each point $ijkl$ is computed as shown in Figure 5.

$$(\nabla\zeta \cdot \nabla\zeta)_{ijk} = \frac{1}{4} \left\{ \begin{aligned} & \left[\frac{1}{\Delta x} (\zeta_{i+1,j,k} - \zeta_{i-1,j,k}) \right. \\ & \quad \left. + \frac{\Delta x}{(\Delta x^2 + \Delta y^2)} \{ (\zeta_{i+1,j+1,k} - \zeta_{i-1,j-1,k}) + (\zeta_{i+1,j-1,k} - \zeta_{i-1,j+1,k}) \} \right]^2 \\ & + \left[\frac{1}{\Delta y} (\zeta_{i,j+1,k} - \zeta_{i,j-1,k}) \right. \\ & \quad \left. + \frac{\Delta y}{(\Delta x^2 + \Delta y^2)} \{ (\zeta_{i+1,j+1,k} - \zeta_{i-1,j-1,k}) + (\zeta_{i-1,j+1,k} - \zeta_{i+1,j-1,k}) \} \right]^2 \\ & + \left[\frac{1}{\Delta z} (\zeta_{i,j,k+1} - \zeta_{i,j,k-1}) \right. \\ & \quad \left. + \frac{\Delta z}{(\Delta x^2 + \Delta z^2)} \{ (\zeta_{i+1,j,k+1} - \zeta_{i-1,j,k-1}) + (\zeta_{i-1,j,k+1} - \zeta_{i+1,j,k-1}) \} \right]^2 \end{aligned} \right\}$$

Figure 5. Scalar dissipation algorithm for computing $\nabla\zeta \cdot \nabla\zeta(\mathbf{x}, t)$ at any point (i, j, k) from the measured conserved scalar field $\zeta(\mathbf{x}, t)$. Here the values of the dissipation obtained in each of four coordinate orientations achieved by rotations in the (x-y) and (x-z) planes are equally weighted, with no particular orientation being preferred.

Example Measurement

As an example, we present here results for the conserved scalar and resulting scalar dissipation rate fields in the self-similar far field ($x/d = 235$) of an axisymmetric turbulent jet at $Re = 6,000$. In this relatively simple case, the four-dimensional data space consisted of 50 successive three-dimensional spatial data volumes, each consisting of 5 parallel spatial data planes. The $(1/e)$ laser beam thickness was measured as $380 \mu\text{m}$, while the resolution Δz between spatial data planes was $220 \mu\text{m}$. With an image ratio of 2.89, the in-plane resolution was $\Delta x = \Delta y = 116 \mu\text{m}$. These values can be compared with the strain-limited diffusion scale estimate of $\lambda_D \approx 407$

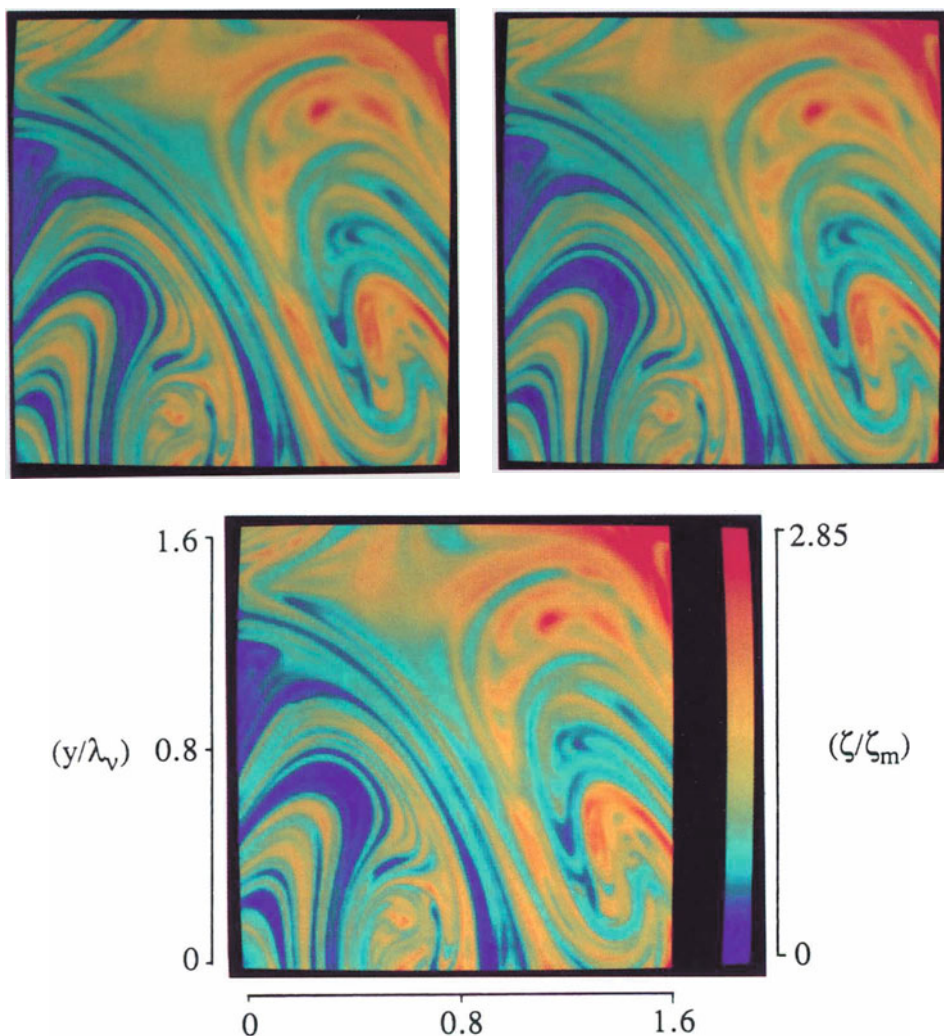


Fig. 6. The measured $Sc \gg 1$ conserved scalar field $\zeta(\mathbf{x},t)$ in three typical adjacent 256×256 spatial data planes (x,y) from a typical three-dimensional spatial data volume (x,y,z) from a measured four-dimensional data space (x,y,z,t) . The measurements shown were obtained at $Re = 6,000$ in the fully-developed self-similar far field ($x/d = 235$) of an axisymmetric turbulent jet. The scale indicates the spatial extent of the data relative to λ_v . The 256 different colors identify the local 8-bit value of the measured scalar field, with the color bar giving the conserved scalar values relative to the local mean value ζ_m . The three spatial data planes are shown in order of increasing z (and therefore increasing t) in the clockwise direction, beginning at the upper left. The spatial resolution (Δx , Δy) within each data plane and (Δz) between adjacent data planes, as well as the temporal resolution between adjacent three-dimensional data volumes, is sufficiently fine relative to the local strain-limited molecular diffusion scale estimate to allow accurate differentiation of the data in all three spatial dimensions and in time. This allows determination of the true local instantaneous scalar energy dissipation rate field $\nabla\zeta \cdot \nabla\zeta(\mathbf{x},t)$ in Eqs. (1) and (2) through the four-dimensional data space, as shown in Fig. 7.

μm . Note that the resulting pixel image volume was nearly 23 times smaller than the estimated local strain-limited molecular diffusion volume λ_D^3 , with its maximum dimension nearly 2 times smaller than λ_D . Similarly, the time between successive data planes was $\Delta t = 9.0$ msec while the time lapse between the same data plane in successive data volumes was $\Delta T = 45$ msec, both of which are significantly less than the estimated local diffusion scale passage time $(\lambda_D/u) \approx 100$ msec.

Figure 6 shows the 8-bit conserved scalar data in three typical parallel adjacent 256×256 spatial data planes from the same data volume. The color levels denote the local conserved scalar value $\zeta(\mathbf{x},t)$ at each point, with pure blue corresponding to pure ambient fluid and increasing uniformly to pure red, corresponding to the highest scalar values in the data. Note that, for the conditions in this particular measurement, the data planes shown span approximately $1/17$ of the local flow width $\delta(\mathbf{x})$ in each direction. This suggests that the fine scale mixing process seen within the measured data space will likely display features that are generic to mixing in turbulent shear flows in general, and not specific to just this one particular flow. In Figure 7 we show the true scalar dissipation rate field $\log_e \nabla \zeta \cdot \nabla \zeta(\mathbf{x},t)$ obtained from the data in the three adjacent scalar planes in Figure 6, where the logarithmic form is used simply to allow increased contrast at low dissipation values. In this case, the 256 different color levels denote increasing values of the mixing rate. The first level, colored black, denotes zero and very low mixing rates, while the remaining levels range uniformly from pure blue through pure red and denote logarithmically increasing values of the local instantaneous scalar dissipation rate in the flow. To examine the time evolution of the true molecular mixing rate field, Figure 8 shows the scalar dissipation rate field in the same spatial data plane from four temporally successive three-dimensional data volumes. Note that a technical discussion of some of the implications of results from these four-dimensional measurements for the fine structure of mixing in turbulent flows is given by Dahm, Southerland & Buch (1990).

While this ability to study the evolution of the mixing process is itself very insightful, perhaps the most important difference between these four-dimensional data and the earlier three-dimensional spatio-temporal data of Dahm & Buch (1989, 1990) is the ability to include the third component of the scalar gradient vector in forming the scalar dissipation rate field. In particular, in a two-dimensional approximation of the scalar dissipation, molecular diffusion layers oriented largely parallel to the data plane are not discernible. By comparison, the three-dimensional spatial nature of the present data should capture the complete topology of the dissipation field. Notice also that in Figures 7 and 8, both isolated as well as interacting dissipation layers can be seen. The earlier measurements of Dahm & Buch (1990) have shown that the internal structure of the isolated layers closely matches the self-similar solution for the evolution